

USE OF AN ECR ION SOURCE FOR MASS SPECTROMETRY

D. Button and M.A.C. Hotchkis
ANSTO, PMB 1, Menai, NSW 2234, Australia.

Abstract

At ANSTO we have developed an Electron Cyclotron Resonance (ECR) ion source to investigate new concepts for mass spectrometers designed to measure isotopic ratios of elements such as carbon, nitrogen and oxygen. The low pressure ECR plasma presents particular challenges when used for mass spectrometry. The elements we are interested in measuring are typically present as residual gas in vacuum systems and hence we need to achieve ultra-high vacuum throughout our system. Also ECR plasmas generate highly reactive species of these elements which can then bond to internal surfaces. A number of measures have been taken to combat these difficulties. We have shortened the plasma bottle length to minimise the surface area. In making this change we have also discovered that the useful plasma volume is much less than expected. Originally the source was designed with a mirror ratio of around 2.1. With the restricted bottle size, our effective mirror ratio is 1.8 and yet the performance of the source is unaffected. This and other design modifications will be discussed.

INTRODUCTION

At ANSTO we are developing an Isotopic Ratio Mass Spectrometer (IRMS) system utilising an Electron Cyclotron Resonance Ion Source (ECRIS) [1]. The ECRIS properties have two main advantages over traditional systems based on electron impact ionization. Firstly the ionization efficiency which can be 2 orders of magnitude greater than electron impact ionization at converting the sample to an ion beam for measurement. Secondly the process of creating charge states greater than 1+ breaks up molecules which cause molecular interferences in mass spectrometry of the single charge state. For this reason our IRMS system typically makes measurements of 2+ charge state ions, and thus the name adopted for our system is the IRMS++.

Initial testing of the system has verified the ability of our ECRIS to generate 2+ and greater charge states free of molecular interference at a sample efficiency >10%. Other characteristics that are not desirable for the operation of a mass spectrometer have also been discovered. This has included high backgrounds, high levels of background beams and retention of the sample in the ion source (ion source memory effect). We describe below methods used to minimise these effects and modifications that have been made to the ion source to reduce them, while avoiding any negative impact on the performance of the ECRIS.

EXPERIMENTAL ARRANGEMENT

The configuration of the IRMS++ instrument developed at ANSTO is shown in Figure 1, including an electrostatic analyser which has been installed since the work shop report ref[1]. The system incorporates an in house developed cost effective ECR ion source to produce low to medium charge state ions. The source is described briefly below; a more detailed description of it can be found in a recent paper [2].

Microwave power to the ECR ion source is provided by a 100 watt microwave amplifier and oscillator, which is tuneable within 64 channels across a frequency range of 6.85 – 7.15GHz. The microwave generator is coupled to the ion source chamber via a wave guide. Normally the microwave generator is operates at 10-25W, and frequency of 7.115GHz.

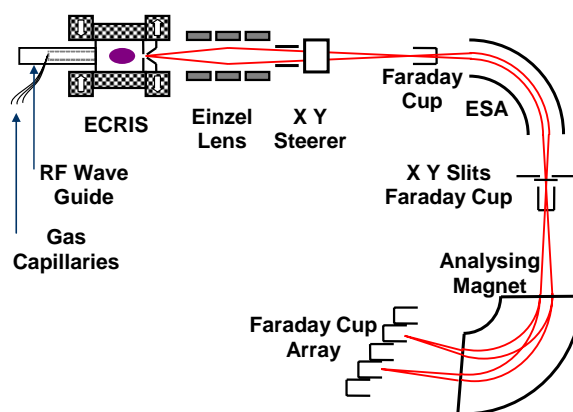


Figure 1: The configuration of the ANSTO IRMS++ instrument.

The magnet field is achieved by permanent magnets, consisting of 2 ring magnets to form the axial field, and a hexapole to form the radial field.

The plasma bottle is constructed from a 48mm ID closed end quartz tube, with the closed end transitioning to a 9mm OD tube as to deliver gas to the plasma chamber. The quartz plasma bottle is transparent to microwaves enabling the capping of the end, and provides electrical isolation to ground for the plasma electrode and the plasma itself. The support, and sample gases are delivered to the 9mm OD quartz tube via 3 polymer coated silica capillaries of different lengths and diameters, allowing delivery of gases from chambers at pressures ranging from 5 to 1000 Torr. These utilise the poor conductance to transition between laminar gas flow in the sample section, to molecular flow of the Ultra High

Vacuum (UHV) ion source without fractionating the sample.

The plasma electrode has a 2.5mm diameter aperture, and was constructed from stainless steel which was later electroplated with gold to ensure an inert surface. Efficient utilisation of the sample gas is enhanced by an aluminium foil seal between the circumference of the plasma electrode and the quartz wall of the plasma bottle. Post extraction the system incorporates an einzel lens, followed by X and Y steerers. Beams are energy-analysed with the electrostatic analyser and separated according to their mass to charge ratio in the analysing magnet. Multiple beams can be measured simultaneously by the Faraday Cup array.

The UHV system is oil free, and consists of 2 150 l/sec turbo molecular pumps (both have 2 greased bearings) backed by a 14m³/h 5 stage roots blower pump, which itself backed by a 2 stage diaphragm pump. The first Turbo pump is located on the einzel lens chamber directly after the source, and the second on the electrostatic analyser chamber. A 60l/sec triode ion pump is located on the Faraday cup array chamber. This configuration allows use to regularly achieve base pressures $<4 \times 10^{-6}$ Pa.

HIGH BACKGROUNDS AND CONTAMINATION

As the IRMS++ system is intended for the measurement of isotopic ratios of oxygen, carbon, and nitrogen in substances such as water carbon-dioxide, nitrogen gas, etc. it is imperative that the residual sources of these species be minimized in the system. In our earlier paper [2], we showed results where low backgrounds were achieved, with total contamination beams at around 0.2% of the total beam. However, this level proved to be very hard to achieve on a routine basis. Figure 2 show a typical mass spectrum captured from 5N (99.999%) purity helium. The spectrum indicates oxygen, hydrogen, and carbon peaks of the order of hundreds of nanoamps, compared to just over 10 μ A of helium beam. The relatively low level of nitrogen beams shows that air leaks are not a major factor in this instance. Possible sources of the contamination include water vapour, oxygen, hydrocarbons, hydrogen and carbon from stainless steel, and others. Possible processes leading to the release of contaminants include outgassing, permeation, diffusion through capillaries, desorption, and others. While some of these effects relate simply to the technicalities of vacuum practice, there are also significant effects peculiar to the use of a plasma. The plasma may both cause deposition on the walls and strip and recycle materials from the chamber walls. Such effects are well known in a number of areas of technology (see for example, ref [3]). However, the ECR ion source is an unusual environment and our requirements are particularly stringent.

Surface deposits and the cleaning process for the ion source bottle

The background was firstly considered to originate from residual contaminants from the cleaning of the quartz ion source bottle.

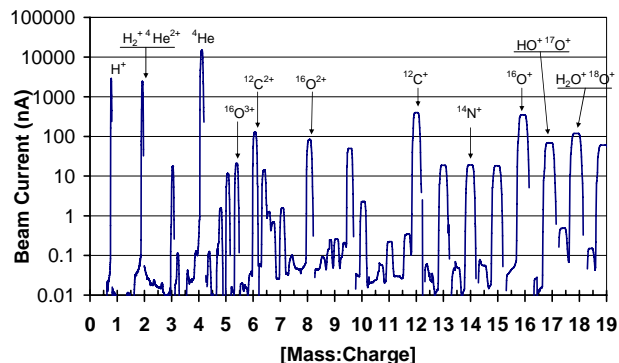


Figure 2: Above is a typical mass spectrum generated from running helium support gas.

In one attempt to remove oxide layers from the internal surfaces of the plasma chamber, cyclohexane (C₆H₁₂) vapour was introduced into the plasma. However, perhaps not surprisingly, this led to undesirable and persistent residual carbon beams. The source was opened to clean it. Figure 3(a) shows the pattern of contamination on the plasma bottle, including obvious carbon deposits. The pattern, while quite familiar to ECR ion source users, demonstrates how the plasma has a strong cleaning effect in the principal electron loss zones, but leaves deposition areas just adjacent to this zone. We believe this evidence provides an important clue as to the deposition/desorption processes occurring in the chamber with all types of sample gases.

It is also worth noting our cleaning procedure for the quartz bottle.

Hydrofluoric acid etching was our original preferred method of cleaning. However, preferential etching at imperfections in the surface of the quartz leaves an undesirably roughened surface finish. Internally, this can increase the surface area for deposition. Externally, the roughening can make it more difficult to achieve a vacuum seal at the ends

As a result of the surface finish from the etching, the procedure was changed to the following 4 step process.

1. Visible deposits are abrasive removed from bottle inner surface.
2. Bottle is cleaned in Aqua regia (1:3 nitric acid to hydrochloric acid) then rinsed with high purity water.
3. The bottle is ultrasonic cleaning in ethanol.
4. Finally the bottle is vacuum baked at 150°C.

The Aqua regia was selected as it dissolves gold and rhodium which could be sputtered from the plasma electrode, as well as other metals. However, some kinds of deposits, eg carbon, are not removed effectively by this method leaving a surface staining.



(a)



(b)

Figure 3: Image (a) shows the residual surface contamination within the plasma bottle after running Cyclohexane (C_6H_{12}) vapour. Image (b) shows the bottle after atmospheric baking at $1000^{\circ}C$ for 2 hours.

Carbon 14 sample preparation for accelerator mass spectrometry requires extremely clean glassware during the chemistry preparation process as to minimise the introduction of modern carbon. At ANSTO this is achieved in the final stage by baking the glassware in a furnace to burn off any carbon residue. For this reason a similar process was introduced as the final step in the ion source bottle cleaning process. This was the baking of the plasma bottle at $1000^{\circ}C$ in an atmospheric furnace for 2 hours. Figure 3 (b) shows the plasma bottle after this baking has been performed. This visually restored the surface to a pristine condition, and gave a visually cleaner surface than the previous methods. This was also evident in the reduction in the conditioning time to achieve base background levels.

Sources of oxygen contamination

As initially intended of the instrument is for the measurement of oxygen ratios we focused on the sources of oxygen in the system via various processes. Table 1 lists the processes of oxygen contribution that were investigated as background sources. Out of those listed in

the table 1, the sources that were found to have a significant contribution are discussed below.

Table 1

	Possible Source of Oxygen Contamination	Effect
1	Oxygen or water vapour contamination in the helium carrier gas.	Significant
2	Oxygen or water vapour contaminant diffusing in through capillaries from sample chambers.	Negligible to None
3	Outgassing of stainless steel fittings at UHV end of capillaries.	Negligible to None
4	Outgassing of ferrules used to seal capillaries.	Significant
5	Outgassing or permeation of elastometer (FKM 'Viton') seal used to join stainless steel fittings to quartz inlet tube on the plasma chamber.	Significant
6	Sputtering of oxygen from quartz surface inside vacuum chamber	Negligible to None
7	Oxygen, water, or oxide layer on the inside of the plasma chamber. This layer is probably created by the action of the plasma, and is only released through the action of the plasma.	Very Significant
8	Diffusion of oxygen or water vapour from residual gas in vacuum in the beam extraction region into the plasma chamber.	Negligible to None

Oxygen or water vapour contamination in the helium carrier gas. The gas flow from the 99.999% helium cylinder was passed through a high surface area stainless steel vacuum bellows, submerged in liquid nitrogen before entering the sample system. This would freeze out any water vapour, carbon dioxide, and possibly liquefy O_2 also. The result was a significant decrease in the overall contamination level. As a result of these findings, a new manifold system for the cylinder gases is under construction, and incorporates Alltech All-Pure gas specific filtering columns [4] for helium and hydrogen, as used in gas chromatography, to remove CO , CO_2 , O_2 , H_2O , and sulphur compounds to $<1ppb$.

Outgassing of ferrules used to seal the capillaries. The heating of the original Vespel [5] ferrules showed a constant outgassing level suggesting a permeation or leak due to the applied heat. Retightening of the ferrule made no impact on this rate. An alternative all metal sealing product for capillaries namely Siltite [5] ferrules were installed in place of the Vespel. Baking of these fittings showed a distinctive outgassing cycle with no sign of an ongoing leak, or permeation.

Outgassing or permeation of elastomer (FKM 'Viton') seal used to join stainless steel fittings to quartz inlet tube on the plasma chamber. This was assessed by baking the fitting to 180°C. It was found that the o-ring of the Swagelok Ultratorr 3/8" fitting would show a standard bake-out curve, which after 24h would have an improved performance. Although after the baking over a week the contamination would show signs of increase. If re-baked the o-ring would again show signs of out gassing demonstrating a standard out gas curve with quite a high initial outgas rate. It was considered that the o-ring was absorbing water from the lab air, and permeating it through to the vacuum side. To verify this process the system was run logging $^{16}\text{O}^{2+}$ currents and the o-ring fitting was wet with water. Figure 4 shows the logged data and the rate at which the oxygen levels increased. To prevent this process the stainless steel fitting was modified and adhered to the quartz with Torr Seal [6] epoxy. This gave an improved performance over the elastomer seal and can also be baked to 120°C. After initial baking of the Torr Seal bond and fitting, the vacuum base pressure doesn't respond again to later heating.

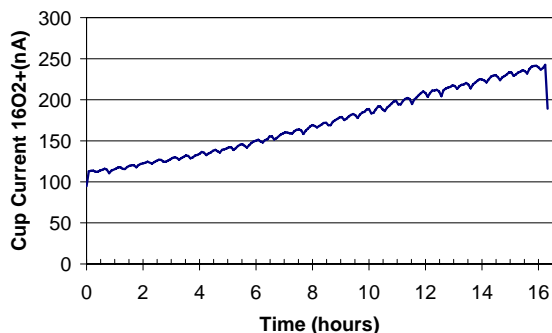
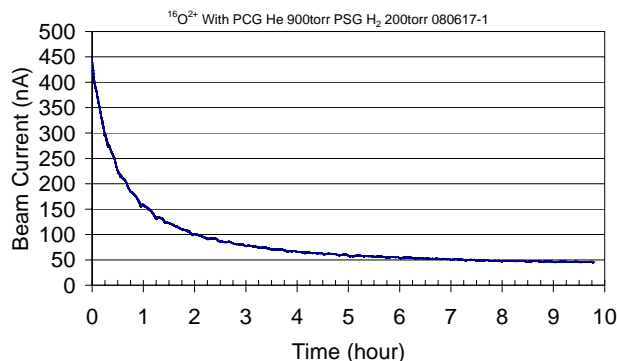


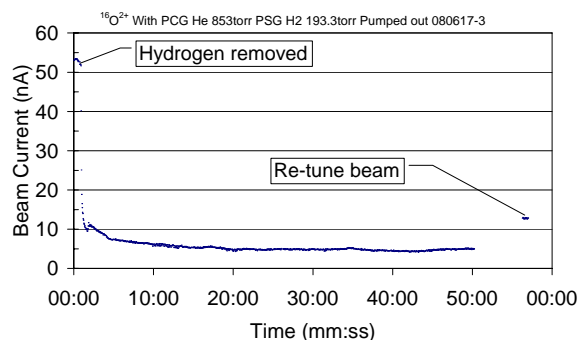
Figure 4: This chart show the increasing $^{16}\text{O}^{2+}$ background over 16 hours due to the wetting of the FKM 'Viton' o-ring of the Ultratorr fitting. The fitting couples the quartz gas delivery tube of the ion source bottle to stainless steel fittings which interfaces the capillaries from the sample from the sample chamber.

Oxygen, water, or oxide layers on the inside of the plasma chamber. Such layers are probably created by the action of the plasma, and are only released through the action of the plasma. To establish that these layers are generated by the plasma, the ion source was run continuously with helium to burn out contaminants to normal background levels. As the magnet array on the ECR ion source is mounted on liner bearings, the location of the ECR zone and associated loss zones of the ion source are able to be moved relative to the plasma chamber. Utilising this ability the magnet array was moved 5-10mm after achieving base background levels, the source showed an immediate increase in contamination levels. Leaving the array in the offset position, the source was once again left to burn out the

contaminants to background levels. The array was relocated to the original position once again, with the background contamination levels once again immediately elevating. As the contaminants may tend to deposit out around the plasma bottle as like those shown in figure 3(a), it was considered that an in situ surface cleaning process was required.



(a)



(b)

Figure 5: Chart (a) shows the reduction in the $^{16}\text{O}^{2+}$ beam over a period of 10 hours after the introduction of hydrogen into the ion source. Chart (b) shows the reduction in the $^{16}\text{O}^{2+}$ over 1 hour after the removal of the hydrogen.

Hydrogen gas was chosen for this purpose, as it may be expected that hydrogen atoms or ions can bonds with contaminants mobilising them as gasses molecules. Once liberated from the surface the contaminant can re-enter the plasma or be pumped away. Figure 5(a) shows the decay of the $^{16}\text{O}^{2+}$ beam after the introduction of hydrogen in addition to the helium in the ion source. Figure 5(b) shows the $^{16}\text{O}^{2+}$ beam after the hydrogen was removed from the sample system, which further reduces the level of $^{16}\text{O}^{2+}$ in the beam. Note after an hour the beam optics were retuned to show the true $^{16}\text{O}^{2+}$ level. The drop in the $^{16}\text{O}^{2+}$ beam after the removal of the hydrogen further demonstrates the dependence of the hydrogen at liberating the contaminant. There is clearly a very considerable reduction to the oxygen surface contamination of the plasma bottle. Although this was not the first time that hydrogen had been run in the ion source, the effectiveness for cleaning was not noticeable

until the before mentioned background reduction modifications had been made.

Figure 6 shows the resulting spectrum against the original spectrum after the above modifications and cleaning processes.

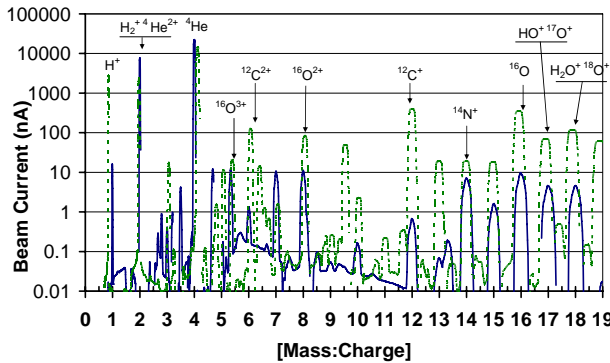


Figure 6: This chart show the background after the modifications, and cleaning of the system.

ION SOURCE RETENTION

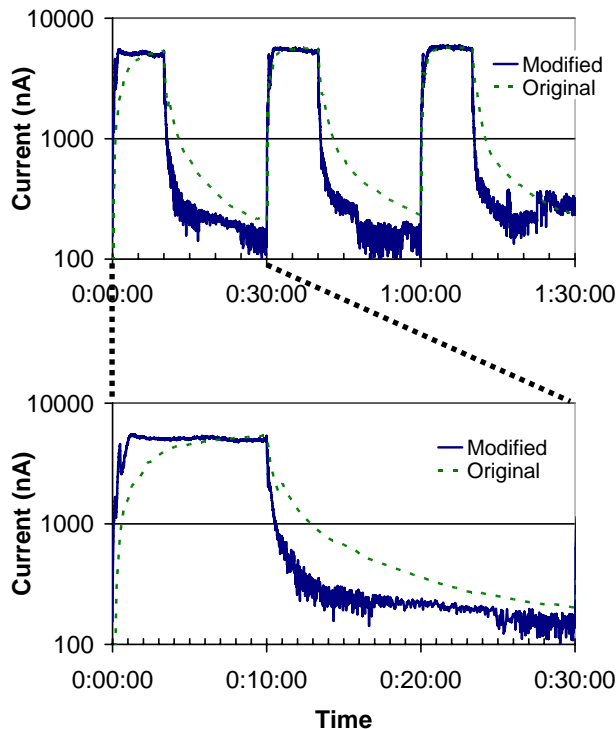


Figure 7: The chart shows the original, and modified ions source rise and delay characteristics of $^{14}\text{N}^{2+}$ beam over 3 cycles of nitrogen gas introduced for 10 minutes, then pumped away for 20 minutes.

Initial testing of the instrument indicated that there was a significant rise and decay time during the introduction and removal of sample gases [2]. This can be seen in Figure 7, demonstrating this effect within a $^{14}\text{N}^{2+}$ beam. It was also found that the instrument vacuum, as measured

in the flight tube after the einzel lens, also reflected the same rise and decay characteristic over the same period. It was considered that the capillary lines after transferring the gas to the ion source from the sample section, can act as a storage volume that releases slowly due to the low conductance of the capillary. Varying the length of the capillaries thus their volume, had no impact on the rise and decay rates of the beam.

Dummy runs of the sample pulses into the source, with the microwave unit turned off thus plasma extinguished, showed that the vacuum of the system responded at a much faster rate, coming to equilibrium within 10 seconds of introduction and removal of sample gases. It was also found that when the source was ignited after the dummy run, that there was no residual background in the ion source due to the recently introduced sample gas.

During both the rise and decay portion of a sample cycle, the RF source was turned off to allow the vacuum level to reach the peak and base values before restarting the RF. When the plasma was reignited, in both cases the vacuum and beam currents returned to the previous point in the rise and decay cycle. This indicated that the sample gas is stored and removed from the source by the action of the plasma.

Operation of the source with inert gases showed a much faster rise and decay cycle taking 10s of seconds to peak and reduce to background as opposed to the 10s of minutes for the reactive gases. For this reason it was thought that there maybe a reactivity problem with the walls of the plasma chamber. To change the plasma chamber wall reactivity, the plasma bottles inner cylinder surface was gold plated by evaporation. The result of this coating did not have a significant effect on the rise and decay period.

An axial sample gas delivery tube was installed in the ion source to try and deliver the gases to the rear edge of the ECR zone. This was to maximise likelihood of the first interaction of the sample gas to be ionization as opposed to molecular interaction with the surfaces of the plasma chamber. This did not show any benefit to the rise and decay rate, but did show that we were able to place a surface beyond the B_{max} point of the axial field towards the ECR zone without degrading the operation of the ion source.

As the retention process appeared to be an effect that takes place between the plasma chamber surface and the plasma, it was consider that reducing the available surfaces in the ion source chamber could reduce the effect. Figure 3(a) also shows that there is a cleaning effect from bombardment of the inner quartz surfaces at the loss zones, this can be seen as the transparent area surrounded by the carbon residue, this feature is also found on the plasma facing electrode. Thus an increase in the ratio of area interacting with the lose zones, to those inactive areas outside of them is desirable.

To achieve a reduced inactive surface area in the ion source, the plasma facing electrode was moved toward the ECR zone within the hexapole between the resonance field of 0.25T and the B_{max} of 0.456T, residing at 0.390T.

The length of the plasma bottle was also reduced so that the back of the plasma bottle finished at the geometric symmetrical location to the hexapole with an axial field strength of 0.425T. These modifications can be seen in figure 8, which shows the relative source component locations to the axial field strength.

This modification didn't inhibit the operation of the source, but effectively altered the mirror ratio (B_{\max} / B_{\min}

on the axis) at the inlet and extraction ends of the ion source. The extraction end reduced from 2.10 to 1.81, and the inlet end reduced from 2.4 to 1.98. As a larger mirror ratio is conventionally considered to facilitate the generation of higher charge state ions, it was of importance to verify the effect of this modification on the charge state distribution performance.

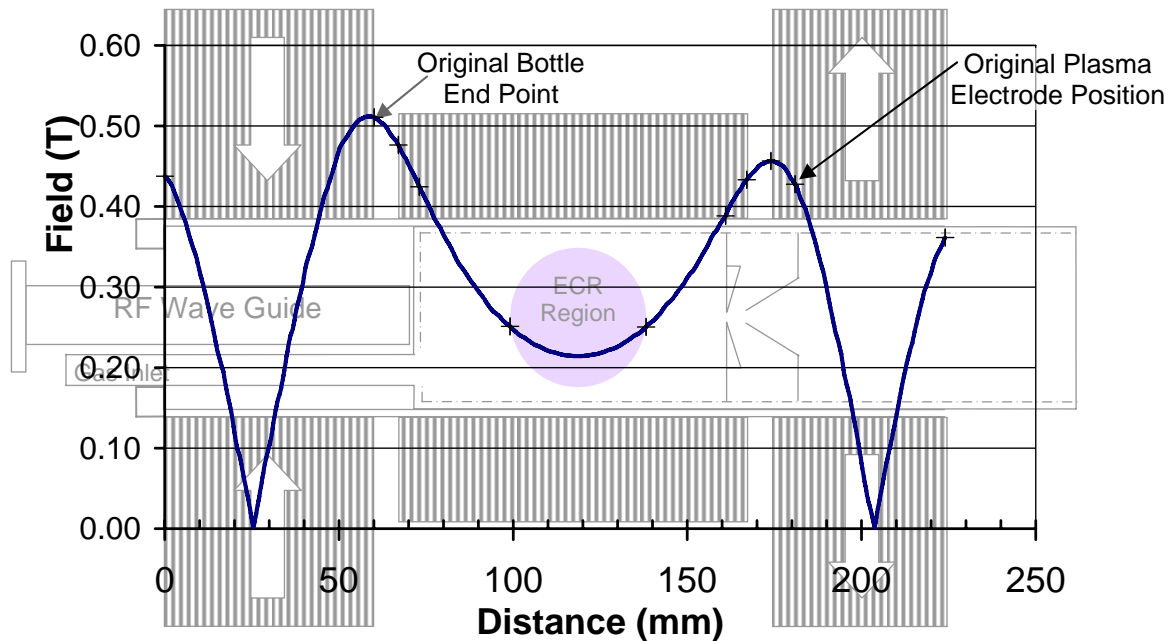


Figure 8: The above is a plot of the axial field of the ECR magnet array. The relative positions of the various elements of our ion source can be seen with respect to the field structure. Note that the plasma facing electrode, and end of the quartz plasma bottle are located on the ECR zone side of their respective B_{\max} .

Figure 9 shows the charge state distributions of the nitrogen ion charge states for both helium supported, and pure nitrogen for both the original source geometry, and modified geometry. The chart shows that there is little effect on the distribution, and no degrading of the 2+ charge state which is utilised for the measurement of oxygen isotopic ratios.

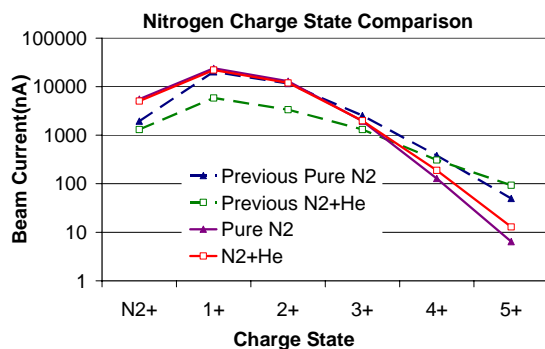


Figure 9: Plot shows the beam current of each of the charge states of nitrogen produced by the ion source with the original geometry, and the compacted geometry.

Applications and Diagnostics

REFERENCES

- [1] M.A.C. Hotchkis, D. Button, C.L. Waring, Rapid Comm. Mass Spectrom. 22 (2008) 1408.
- [2] M.A.C. Hotchkis, Buckley D, Button D. Rev. Sci. Instrum. 79 (2008) 02A304.
- [3] K. S. A. Butcher, Afifuddin, P. P.-T. Chen, and T. L. Tansley, phys. stat. sol. (c) 0 (2002) 156.
- [4] Supplied by <http://www.discoverysciences.com>
- [5] Supplied by SGE <http://www.sge.com/>
- [6] Supplied by Varian <http://www.varianinc.com>